Carbohydrate Polymers 117 (2015) 813–817

Contents lists available at ScienceDirect

Carbohydrate Polymers

journal homepage: www.elsevier.com/locate/carbpol

Facile preparation of silver nanoparticles immobilized on chitin nanofiber surfaces to endow antifungal activities

Shinsuke Ifuku[a,*], Yui Tsukiyama[a], Taisuke Yukawa[a], Mayumi Egusa[a], Hironori Kaminaka[b], Hironori Izawa[a], Minoru Morimoto[c], Hiroyuki Saimoto[a]

[a] Department of Chemistry and Biotechnology, Graduate School of Engineering, Tottori University, 4-101 Koyama-cho Minami, Tottori 680-8552, Japan
[b] Faculty of Agriculture, Tottori University, 4-101 Koyama-cho Minami, Tottori 680-8553, Japan
[c] Research Center for Bioscience and Technology, Tottori University, 4-101 Koyama-cho Minami, Tottori 680-8550, Japan

ARTICLE INFO

Article history:
Received 29 August 2014
Received in revised form 14 October 2014
Accepted 17 October 2014
Available online 30 October 2014

Keywords:
Chitin
Nanofiber
Silver nanoparticle
Light absorption
Antifungal

ABSTRACT

Silver nanoparticles were prepared on chitin nanofiber surfaces by UV light reduction of silver ions. The chitin nanofibers could be efficient substrates to immobilize silver nanoparticles with stable dispersion states. The dispersion and the nanocomposite film with acrylic resin showed characteristic absorption property in the visible light region due to the effect of the silver nanoparticles. Silver nanoparticles endowed strong antifungal activity to chitin nanofibers.

1. Introduction

Understanding of the nanostructured chitin fiber in marine organisms enables new approaches to the production of novel materials of biomedical interest capable of enhanced properties. Electrospinning, intended to impart large superficial specific area to manufactured chitin/chitosan materials, is also being developed (Muzzarelli, 2011, 2012).

Recently, we have prepared chitin nanofibers (n-chitin) from crab (Ifuku, Nogi, et al., 2009) and prawn shells (Ifuku, Nogi, et al., 2011) as well as from mushroom cell walls (Ifuku, Nomura, Morimoto, & Saimoto, 2011) by a simple mechanical disintegration treatment (Ifuku & Saimoto, 2012). N-chitins have a highly uniform structure with approximately 10 nm thickness and excellent mechanical properties due to their anti-parallel extended crystalline structure. Although commercially available chitin is insoluble and precipitates in water, n-chitins can disperse homogeneously. Thus, the dispersion is easy to handle and to shape into desired forms depending on the applications. Moreover, we have reported powerful biological activities of n-chitins. For example, n-chitins showed anti-inflammatory actions by suppressing NF-κB and MCP-1 activations, and suppressed fibrosis in an acute ulcerative colitis mouse model (Azuma, Osaki, Wakuda, et al., 2012; Azuma, Osaki, Ifuku, et al., 2012). n-Chitins are potentially useful in novel medicines or in functional foods for patients with inflammatory bowel disease. Moreover, n-chitin improved the epithelial granular layer, increased granular density, and resulted in a reduced production of TGF-β (Ito et al., 2014). Thus, n-chitin can be incorporated into cosmetics or textiles. Consequently, we expect that n-chitin with those biological properties will find increased application in biomedical fields. However, n-chitins do not have specific anti-bacterial properties (Ifuku et al., 2013).

Silver nanoparticles (nAgs) have received much attention as efficient antimicrobial agents (Sondi & Salopek-Sondi, 2004; Rai, Yadav, & Gade, 2009). Their extremely high surface area offers better contact with microorganisms. nAgs penetrate inside the bacteria and interact with proteins in the cell, leading to cell death. It is generally difficult to disperse nAgs in a solvent, since the nanoparticles form aggregates due to their high surface energy. Some researchers have reported that stable aqueous dispersions of nAgs can be prepared by a reduction of silver ions in the presence of a stabilizing agent. On the other hand, there has been no report about nAgs immobilized on n-chitins. Here, we demonstrate a facile fabrication of nAgs on an n-chitin surface, which can behave as a substrate to stabilize nanoparticles. And we investigate the antibacterial property of the nAgs/n-chitin composite. Although there have

* Corresponding author. Tel.: +81 857 31 5592; fax: +81 857 31 5813.
E-mail address: sifuku@chem.tottori-u.ac.jp (S. Ifuku).

http://dx.doi.org/10.1016/j.carbpol.2014.10.042
0144-8617/

been several articles about immobilization of nAgs on chitosan and cellulose nanofibers (Ifuku et al., 2009a; Ifuku, Tsuji, et al., 2009b; Lee et al., 2014), chitosan itself has already antimicrobial activity in nature and cellulose basically does not have above described bioactivities. Thus, endowing the antifungal property to n-chitin with several biological properties is important to expand its commercial applications.

2. Experimental

2.1. Materials

Chitin powder from crab shells was purchased from Koyo Chemical. Tricyclodecane dimethanol dimethacrylate, a methacrylic monomer, was obtained from Shin-Nakamura Chemical. Other chemicals were purchased from Wako Pure Chemical Industries and TCI Fine Chemicals, and were used as received.

2.2. Preparation of silver nanoparticles immobilized on chitin nanofibers

n-Chitins were prepared as described previously with some modification (Dutta et al., 2013). Dry chitin powder was dispersed in water at 1.0 wt%. Acetic acid was added to the chitin dispersion to adjust the pH to 3. It was passed through a grinder (MKCA6-3; Masuko Sangyo Co., Ltd.) at 1500 rpm twice. The roughly crushed chitin dispersion was diluted with distilled water to a chitin content of 0.1 wt%. The dilution was passed through a high-pressure water-jet system (Star Burst Mini, HJP-25001 S, Sugino Machine Co., Ltd.) equipped with a ball-collision chamber for mechanical disintegration. Thirty cycles of the treatment were employed for nano-fibrillation. The thus-obtained n-chitin dispersion (90 mL) with 0.1 wt% concentration was mixed with $AgNO_3$ aqueous solution (10 mL). The mixing ratios of $AgNO_3$ to n-chitin were adjusted to 1:9 and 5:9 by weight. For the reduction of silver cation, the mixtures were exposed to UV light using UV curing equipment (SPOT CURE SP-7, Ushio Inc.) at 40 mW cm^{-1} for 0–5 min.

2.3. Preparation of nAg/n-chitin/acrylic resin composite film

The above-prepared 100 mL of nAg/n-chitin water dispersion at a concentration of 0.1 wt% was vacuum-filtered using a hydrophilic polytetrafluoroethylene membrane filter (Millipore, pore size: 0.2 μm) and washed with distilled water and ethanol. The obtained nAg/n-chitin sheet was hot-pressed at 100 °C for 20 min to obtain a dried sheet. The dried sheet was cut into 3 cm × 3 cm sheets, which were impregnated with bi-functional acrylic resins (tricyclodecanedimethanoldimethacrylate (DCP)), with 3 wt% of 2-hydroxy-2-methylpropiophenone photoinitiator under reduced pressure for overnight. The resin-impregnated sheets were polymerized using UV curing equipment (SPOT CURE SP-7, Ushio Inc.) for 10 min at 40 mW cm^{-1}. n-Chitin content of the composite film was approximately 25%.

2.4. Characterization of silver nanoparticles immobilized on n-chitins

The UV–vis light absorbance spectra of nAgs/n-chitin suspensions with a concentration of 0.1 w/v% and the acrylic resin composite films were measured using a UV-Vis spectrophotometer (V550; JASCO).

For field emission scanning electron microscopic (FE-SEM) observation, the prepared nAgs/n-chitin dispersion was diluted with EtOH and dried in an oven to obtain a cast film. The sample was coated with an approximately 2 nm layer of Pt by an ion sputter coater and observed by FE-SEM (JSM-6700F; JEOL, Ltd.) operating at 2.0 kV.

For scanning probe microscopic (SPM) observation, chitin nanofiber slurry was dispersed in water at a concentration of 0.1 mg/mL by an ultrasonic homogenizer for 1 min. A few drops (40 μL) of the suspension was spread on a freshly cleaved mica round disk, dried, and subjected to SPM observation. The SPM observations were performed with an SPM apparatus (Nanocute, SII Instruments).

The X-ray diffraction profiles of the NFs were obtained with Ni-filtered CuKα from an X-ray generator (Ultima IV, Rigaku) operating at 40 kV and 30 mA. The diffraction profile was detected using an X-ray goniometer scanning from 5° to 85°.

2.5. Antifungal activity test

Plant pathogenic fungi were maintained on potato dextrose agar (Difco) slopes or as 15% glycerol stocks at 80 °C. For antifungal activity tests, spores of *Alternaria alternata*, *Alternaria brassicae*, *Alternaria brassicicola*, *Bipolaris oryzae*, *Botrytis cinerea*, and *Penicillium digitatum* were prepared as previously described (Johnson et al., 2000). Spores of *Colletotrichum higginsianum* and *Colletotrichum orbiculare* were obtained as described (Parada, Murakami, Shimomura, Egusa, & Otani, 2011). Spores of *Fusarium oxysporum* f. sp. *lycopersici* and *Pyricularia oryzae* were obtained as described (Ueno, Shibata, Kihara, Honda, & Arase, 2003; Takahashi et al., 2005). A spore suspension (10^5 spores/mL) was dropped onto nAg/n-chitin films. This suspension was placed on a n-chitin as a control. After incubation for 24 h or 7 days, spore germination was observed under a light microscope.

3. Results and discussion

The reduction of Ag^+ was carried out by UV irradiation of $AgNO_3$ and an n-chitin mixture at a concentration of 1 wt%. The mixing ratios of $AgNO_3$:n-chitin (w/w) were 1:9 and 5:9. Fig. 1 shows the UV–vis absorbance spectra after 0–5 min reductions of the dispersion. The $AgNO_3$/n-chitin mixtures were still dispersed homogeneously in water after UV irradiation, and the color changed drastically to brown. The change is obviously due to the surface plasmon resonance of nAgs (Wu, Kuga, & Huang, 2008). Thus, UV irradiation was effective for the reduction of silver ions. The characteristic absorption band was observed mainly at 420 nm and 510 nm. And the absorption intensity increased until 5 min, indicating that the number of produced nAgs increased depending on the reduction time. Moreover, the absorption intensity of the reduced $AgNO_3$/n-chitin mixture with a 5:9 mixing ratio was considerably higher than that of 1:9, indicating that the ratio also affected the amount of nAgs.

Fig. 2 shows SEM and SPM images of the nAgs/n-chitin composite. In the SEM images, nanofibers approximately 10 nm thick were observed after reduction treatment of silver ions, indicating that the UV irradiation process did not affect the characteristic morphology of the n-chitins (Fig. 2a). In a higher-magnification image (Fig. 2b), a number of nanosized bright particles were observed on nanofibers, compared to original n-chitin (Dutta et al., 2013). They were obviously nAgs. The silver ions were reduced by UV irradiation and formed grain aggregates on n-chitin, resulting in fine nAgs. The nAgs seem uniform in size, at approximately 10 nm. However it is difficult to measure the specific sizes of nAgs by FE-SEM due to limited resolution. SPM was also used for nAgs/n-chitin observation (Fig. 2c and d). From the height profile of the SPM image (Fig. 2d), the diameter of nAg was estimated to be approximately 10 nm, which is similar to that observed by the SEM image. These

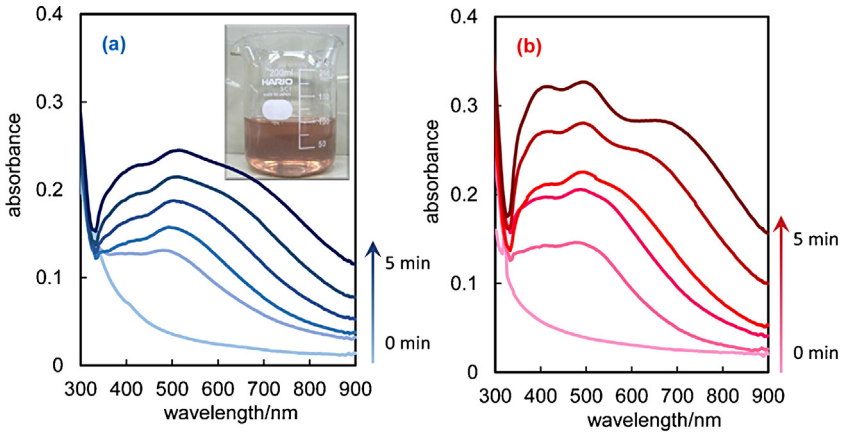

Fig. 1. Effect of irradiation time from 1 to 5 min on UV–vis absorbance spectra of nAgs/n-chitin dispersions with 0.1 wt% concentration. Mixing ratios of $AgNO_3$:n-chitin (w/w) were (a) 1:9 and (b) 5:9.

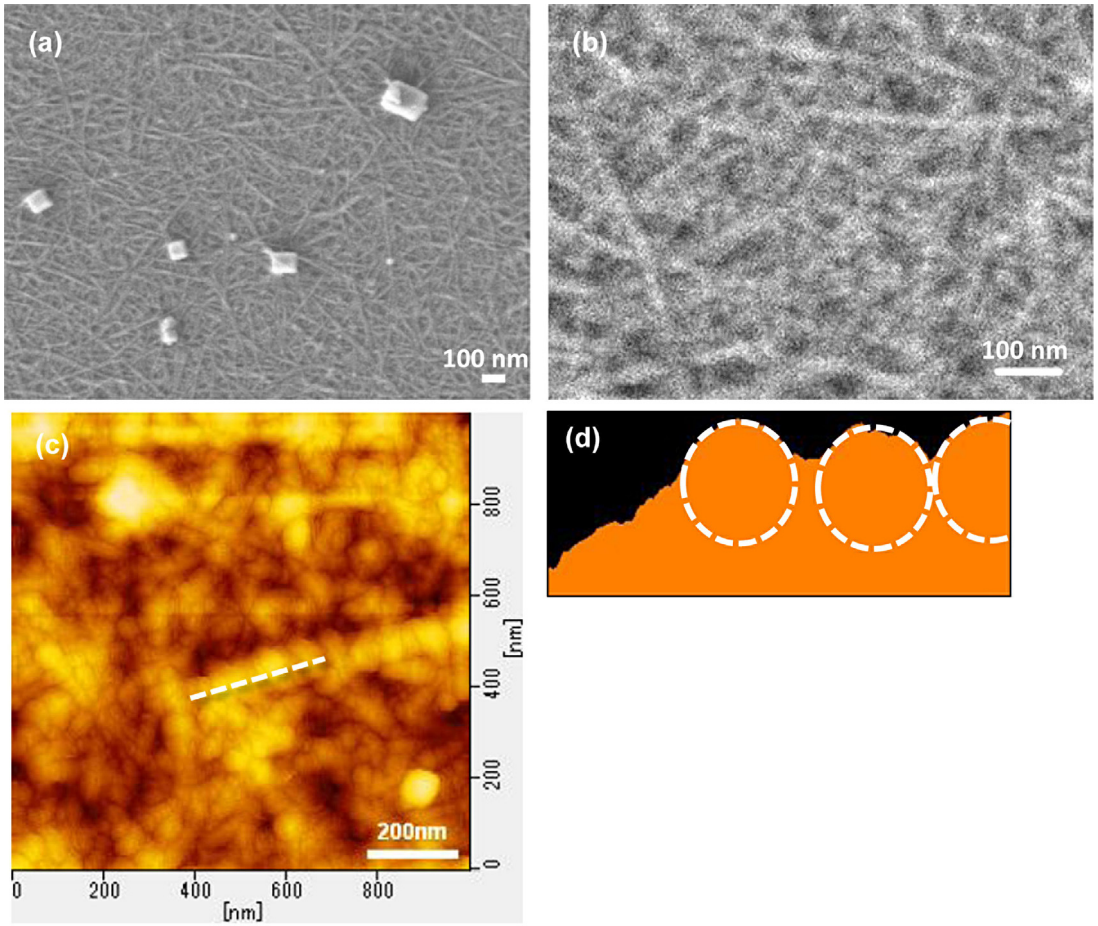

Fig. 2. (a and b) SEM images and (c) SPM image of nAgs/n-chitin nanocomposite with a height profile scanned on the dashed line.

results show that n-chitin can be an effective substrate for stable immobilization of nAgs and stable dispersion in water.

Fig. 3 shows the X-ray diffraction profiles of nAgs/n-chitin composites. The mixing ratios of $AgNO_3$:n-chitin (w/w) were (a) 1:9 and (b) 5:9. The patterns were divided into the ranges of 5° to 30° and 30° to 90°, which were derived from chitin and silver crystal, respectively. The three peaks observed at 8.8°, 19.0°, and 23.2° coincided with the typical antiparallel crystal pattern of α-chitin, corresponding to 0 2 0, 1 1 0, and 1 3 0 planes, respectively (Minke & Blackwell, 1978), indicating that the original crystalline structure remained after nAg immobilization. On the other hand, characteristic silver crystal bands were observed at 37.6°, 45.8°, and 77.4° corresponding to 1 1 1, 2 0 0, and 3 1 1 planes, respectively (Xiang & Chen, 2007), indicating that Ag crystals were produced after UV irradiation.

We prepared a nanocomposite film by using nAgs/n-chitins and an acrylic polymer. The film was optically transparent thanks to the nano-size effect of the n-chitins (Yano et al., 2005; Ifuku, Morooka, Nakagaito, Morimoto, & Saimoto, 2011). Since n-chitins were much thinner than the wavelength of visible light, an n-chitin does not

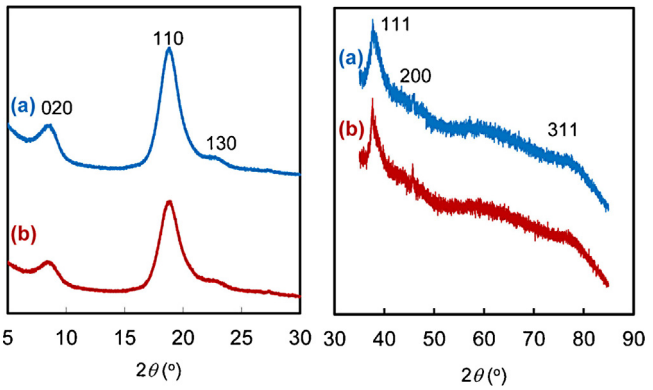

Fig. 3. X-ray diffraction profiles of nAgs/n-chitin composite. Mixing ratios of $AgNO_3$:n-chitin (w/w) were (a) 1:9 and (b) 5:9.

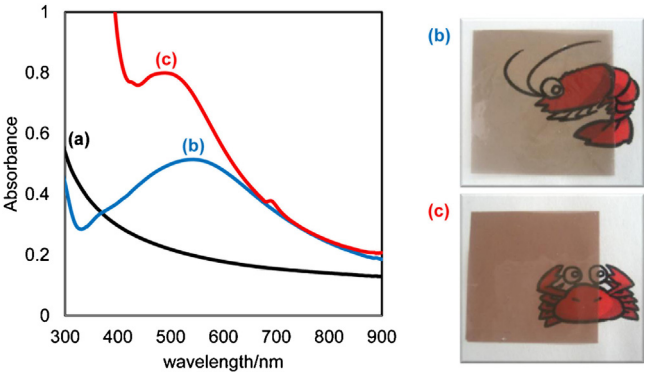

Fig. 4. UV–vis absorbance spectra of n-chitin/acrylic resin composite film (a) without and (b and c) with nAgs and the appearances of the transparent films. Mixing ratios of $AgNO_3$:n-chitin (w/w) were (b) 1:9 and (c) 5:9.

scatter visible light at the interface. Fig. 4 shows the UV–vis absorption spectra of the nanocomposite films and their appearances. The n-chitin/acrylic polymer composite without nAgs had high transparency in the visible region (Fig. 4a). On the other hand, the color of the transparent films became brown by immobilization of nAgs. In the UV–vis spectra in Fig. 4b and c, broad absorption bands were observed with maximum absorbances of 546 nm and 496 nm with mixing ratios of 1:9 and 5:9 ($AgNO_3$:n-chitin), respectively. These band characteristics were apparently due to the surface plasmon resonance of nAgs, corresponding to the brown color (Matsumoto et al., 2006). And the absorption strength of the film with a mixing ratio of 5:9 was higher than that of 1:9, indicating that the amount of loaded nAg with 5:9 was higher than that of 1:9. The nAgs/n-chitins/acrylic resin composite film is available as optical filters which selectively transmit light in a particular range of wavelength.

Table 1 shows the antifungal activity of the nAgs/n-chitin composite film. To assess the antifungal activity, spore germination of plant pathogenic fungi on the films was observed. Spores of all tested fungi germinated on the n-chitins at 24 h, and the n-chitins showed no antifungal activity. The nAgs/n-chitin composite films inhibited the spore germination of almost all tested pathogens at 24 h, and these antifungal activities were sustained at a high degree for 7 days. There was little effect on *B. cinerea*, and the rate of spore germination differed among fungal species, yet the antifungal mechanism of action of silver nanoparticles on each pathogen is unknown. On the other hand, there were no significant differences in antifungal effect between the mixing ratios of 1:9 and 5:9 ($AgNO_3$:n-chitin). These results indicate that nAgs provided strong antifungal activity to chitin nanofibers. However, transparent nAgs/n-chitins/resin composite film did not show antifungal activity, since nAgs were embedded in acrylic resin and were not exposed on the surface of the film.

Table 1
Antifungal activities of nAgs/n-chitin with different mixing ratios of $AgNO_3$:n-chitin (w/w).

Fungi	Rate of spore germination (%)[a]		
	Chitin NF[b]	AgNPs/chitin NF (1:9)	AgNPs/chitin NF (5:9)
A. alternata	93.3 ± 0.5a	15.3 ± 5.4b	4.8 ± 3.8b
A. brassicae	94.8 ± 1.3a	0.5 ± 0.3b	0b
A. brassicicola	91.3 ± 0.5a	1.0 ± 0.4b	0.3 ± 0.3b
B. cinerea	99.3 ± 0.3a	71.8 ± 14.0a	89.9 ± 1.3a
B. oryzae	87.3 ± 2.6a	0.8 ± 0.5b	0.3 ± 0.3b
C. higginsianum	87.8 ± 1.1a	0b	0b
C. orbiculare	97.3 ± 1.3a	0b	0b
F. oxysporum f.sp. lycopersici	99.5 ± 0.3a	2.0 ± 0.7b	0.8 ± 0.5b
P. digitatum	97.8 ± 0.6a	29.8 ± 13.2b	22.5 ± 7.3b
P. oryzae	98.8 ± 0.3a	1.3 ± 0.6b	0.5 ± 0.5b

[a] Data represent the mean of four independent experiments and standard error. Means with the same alphabets are not significantly different according to Tukey's test ($P < 0.05$).
[b] Spore germination was observed after 24 h on Chitin NF, or after 7 days on AgNPs/chitin NF.

4. Conclusion

nAgs were successfully prepared and loaded on n-chitin surfaces by the reduction of Ag ions. Mixing ratios of $AgNO_3$ and UV irradiation time affected the amount of nAgs. n-Chitins can behave as a useful substrate to disperse nAgs stably without coagulation. n-Chitins acquired antifungal properties in addition to various characteristics, such as nano-morphology, high surface area, excellent mechanical properties, and several biological properties. The antifungal property will expand the range of commercial applications of n-chitins in the medical, food, and cosmetics fields.

Acknowledgments

We gratefully acknowledge Dr. Hiroshi Otani (Tottori Univ.), Dr. Sakae Arase (Shimane Univ.), Dr. Tsutomu Arie (Tokyo Univ. of Agr. and Tech.), Dr. Yoshitaka Takano (Kyoto Univ.), and Mr. Kiyotsugu Okada (Osaka Pref. Res. Inst. of Environ., Agri., and Fish.) for providing the fungal strain.

References

Azuma, K., Osaki, T., Wakuda, T., Ifuku, S., Saimoto, H., Tsuka, T., et al. (2012). Beneficial and preventive effect of chitin nanofibrils in a dextran sulfate sodium-induced acute ulcerative colitis model. *Carbohydrate Polymers*, *87*, 1399–1403.
Azuma, K., Osaki, T., Ifuku, S., Saimoto, H., Tsuka, T., Imagawa, T., et al. (2012). α-Chitin nanofibrils improve inflammatory and fibrosis responses in inflammatory bowel disease mice model. *Carbohydrate Polymers*, *90*, 197–200.
Dutta, A. K., Yamada, K., Izawa, H., Morimoto, M., Saimoto, H., & Ifuku, S. (2013). Preparation of chitin nanofibers from dry chitin powder by Star Burst system: Dependence on number of passes. *Journal of Chitin and Chitosan Science*, *1*, 59–64.
Ifuku, S., Nogi, M., Abe, K., Yoshioka, M., Morimoto, M., Saimoto, H., et al. (2009a). Preparation of chitin nanofibers with a uniform width as α-chitin from crab shells. *Biomacromolecules*, *10*, 1584–1588.
Ifuku, S., Tsuji, M., Morimoto, M., Saimoto, H., & Yano, H. (2009b). Synthesis of silver nanoparticles templated by TEMPO-mediated oxidized bacterial cellulose nanofibers. *Biomacromolecules*, *10*, 2714–2717.
Ifuku, S., Nogi, M., Abe, K., Yoshioka, M., Morimoto, M., Saimoto, H., et al. (2011). Preparation of chitin nanofibers with a width of 10–20 nm from prawn shell under neutral conditions. *Carbohydrate Polymers*, *84*, 762–764.
Ifuku, S., Nomura, R., Morimoto, M., & Saimoto, H. (2011). Preparation of chitin nanofibers from mushrooms. *Materials*, *4*, 1417–1425.
Ifuku, S., Morooka, S., Nakagaito, A. N., Morimoto, M., & Saimoto, H. (2011). Preparation and characterization of optically transparent chitin nanofiber/(meth)acrylic resin composites. *Green Chemistry*, *13*, 1708–1711.
Ifuku, S., & Saimoto, H. (2012). Chitin nanofibers: Preparations, modifications, and applications. *Nanoscale*, *4*, 3308–3318.

Ifuku, S., Ikuta, A., Egusa, M., Kaminaka, H., Izawa, H., Morimoto, M., et al. (2013). Preparation of high-strength transparent chitosan film reinforced with surface-deacetylated chitin nanofibers. *Carbohydrate Polymers*, *98*, 1198–1202.

Ito, I., Osaki, T., Ifuku, S., Saimoto, H., Takamori, Y., Kurozumi, S., et al. (2014). Evaluation of the effects of chitin nanofibrils on skin function using skin models. *Carbohydrate Polymers*, *101*, 464–470.

Johnson, R. D., Johnson, L., Itoh, Y., Kodama, M., Otani, H., & Kohmoto, K. (2000). Cloning and characterization of a cyclic peptide synthetase gene from *Alternaria alternata* apple pathotype whose product is involved in AM-toxin synthesis and pathogenicity. *Molecular Plant-Microbe Interaction*, *13*, 742–753.

Lee, S. J., Heo, D. N., Moon, J.-H., Ko, J.-H., Lee, J. B., Bae, M. S., et al. (2014). Electrospun chitosan nanofibers with controlled levels of silver nanoparticles. Preparation, characterization and antibacterial activity. *Carbohydrate Polymers*, *111*, 530–537.

Matsumoto, A., Ishikawa, T., Odani, T., Oikawa, H., Okada, S., & Nakanishi, H. (2006). An organic/inorganic nanocomposite consisting of polymuconate and silver nanoparticles. *Macromolecular Chemistry and Physics*, *207*, 361–369.

Minke, R., & Blackwell, J. (1978). The structure of alpha-chitin. *Journal of Molecular Biology*, *120*, 167–181.

Muzzarelli, R. A. A. (2011). Biomedical exploitation of chitin and chitosan via mechano-chemical disassembly, electrospinning, dissolution in imidazolium ionic liquids, and supercritical drying. *Marine Drugs*, *9*, 1510–1533.

Muzzarelli, R. A. A. (2012). Nanochitins and nanochitosans, paving the way to eco-friendly and energy-saving exploitation of marine resources. *Polymer Science: A Comprehensive Reference*, *10*, 153–164.

Parada, R. Y., Murakami, S., Shimomura, N., Egusa, M., & Otani, H. (2011). Autoclaved spent substrate of hatakeshimeji mushroom (*Lyophyllum decastes* Sing.) and its water extract protect cucumber from anthracnose. *Crop Protection*, *30*, 443–450.

Rai, M., Yadav, A., & Gade, A. (2009). Silver nanoparticles as a new generation of antimicrobials. *Biotechnology Advances*, *27*, 76–83.

Sondi, I., & Salopek-Sondi, B. (2004). Silver nanoparticles as antimicrobial agent: A case study on *E. coli* as a model for Gram-negative bacteria. *Journal of Colloid and Interface Science*, *275*, 177–182.

Takahashi, H., Shimizu, A., Arie, T., Rosmalawati, S., Fukushima, S., Kikuchi, M., et al. (2005). Catalog of Micro-Tom tomato responses to common fungal, bacterial, and viral pathogens. *Journal of General Plant Pathology*, *71*, 8–22.

Ueno, M., Shibata, H., Kihara, J., Honda, Y., & Arase, S. (2003). Increased tryptophan decarboxylase and monoamine oxidase activities induce Sekiguchi lesion formation in rice infected with *Magnaporthe grisea*. *Plant Journal*, *36*, 215–228.

Wu, M., Kuga, S., & Huang, Y. (2008). Quasi-one-dimensional arrangement of silver nanoparticles templated by cellulose microfibrils. *Langmuir*, *24*, 10494–10497.

Yano, H., Sugiyama, J., Nakagaito, A. N., Nogi, M., Matsuura, T., Hikita, M., et al. (2005). Optically transparent composites reinforced with networks of bacterial nanofibers. *Advanced Materials*, *17*, 153–155.

Xiang, Y., & Chen, D. (2007). Preparation of a novel pH-responsive silver nanoparticle/poly(HEMA–PEGMA–MAA) composite hydrogel. *European Polymer Journal*, *43*, 4178–4187.